Biochimica et Biophysica Acta 1837 (2014) 726–733

Contents lists available at ScienceDirect

Biochimica et Biophysica Acta

journal homepage: www.elsevier.com/locate/bbabio

Wavelength dependence of the fluorescence emission under conditions of open and closed Photosystem II reaction centres in the green alga *Chlorella sorokiniana*

Federico Rizzo, Giuseppe Zucchelli, Robert Jennings, Stefano Santabarbara *

Istituto di Biofisica, Consiglio Nazionale delle Ricerche, via Celoria 26, 20133 Milano, Italy
Dipartimento di Bioscienze, Università di Milano, via Celoria 26, 20133 Milano, Italy

ARTICLE INFO

Article history:
Received 20 December 2013
Received in revised form 10 February 2014
Accepted 12 February 2014
Available online 20 February 2014

Keywords:
Maximal photochemical efficiency
Variable fluorescence
Photosystem II
Photochemical yield
Excited state dynamics

ABSTRACT

The fluorescence emission characteristics of the photosynthetic apparatus under conditions of open (F_0) and closed (F_M) Photosystem II reaction centres have been investigated under steady state conditions and by monitoring the decay lifetimes of the excited state, *in vivo*, in the green alga *Chlorella sorokiniana*. The results indicate a marked wavelength dependence of the ratio of the variable fluorescence, $F_V = F_M - F_0$, over F_M, a parameter that is often employed to estimate the maximal quantum efficiency of Photosystem II. The maximal value of the F_V/F_M ratio is observed between 660 and 680 nm and the minimal in the 690–730 nm region. It is possible to attribute the spectral variation of F_V/F_M principally to the contribution of Photosystem I fluorescence emission at room temperature. Moreover, the analysis of the excited state lifetime at F_0 and F_M indicates only a small wavelength dependence of Photosystem II trapping efficiency *in vivo*.

1. Introduction

Photosystem II (PSII) catalyses the light-dependent oxidation of water and the reduction of plastoquinone to plastoquinol. It is composed of two functional moieties: the *core*, which serves both as the photochemical reaction centre as well as the internal antenna, and the external antenna, which only has a light harvesting function. Three principal pigment binding complexes are present in the *core*, CP43, CP47 and the D1–D2 heterodimer that coordinates all the cofactors active in primary photochemistry and successive electron transfer events (*e.g.* [1–6]). The core complex binds about 35 Chlorophyll (Chl) *a* and 12 β-carotene molecules [2,4]. In green plants, the external antenna is composed of several Chl *a*/*b* binding complexes (*e.g.* [5–7]) that also bind oxygenated carotenoids, known as xanthophylls. LHCII is the most abundant complex of the external antenna and is organised as a trimer [5–7]. Typical stoichiometries indicate the presence of three to four LHCII trimers per reaction centres. The other Chl *a*/*b*-binding complexes, CP29, CP26 and CP24, are monomers and are present as a single copy per reaction centre [5–7].

The fluorescence emission of PSII is markedly dependent on the redox state of its terminal electron acceptor (*e.g.* [5–18]), the plastoquinone molecule Q_A (and Q_B). When Q_A is oxidised (reaction centres are said to be in an "open state"), the fluorescence attains the minimal level, F_0, whereas when Q_A is reduced (Q_A^-) the fluorescence emission reaches its maximal level, F_M. Analysis of the excited state decay both in isolated thylakoids and in isolated PSII particles indicates that the average decay lifetimes (τ_{av}) vary as a function of active state of PSII: values in the range of ~300–450 ps (*e.g.* [16–27]) are reported for open states and in the range of ~1–2 ns (*e.g.* [16–22]) for closed reaction centres. Since the change of the average fluorescence lifetime parallels the intensity change observed at steady state, the low fluorescence emission under F_0 condition is interpreted in terms of singlet excited state quenching due to photochemical trapping (photochemical quenching). It is then easily demonstrated that the ratio between the variable fluorescence, $F_V = F_M - F_0$, and the maximal fluorescence level, F_M, represents the maximal quantum photochemical efficiency of PSII, (Φ_{PSII}^{max}) [10,11,14,15]. Values of Φ_{PSII}^{max} fall typically in the 0.75–0.85 interval [8–15].

The F_V/F_M parameter is routinely employed in physiological investigations, particularly under *in vivo* conditions [14,15]. Nevertheless, deriving Φ_{PSII}^{max} from the F_V/F_M ratio is correct only when assuming negligible Photosystem I (PSI) emission in the wavelength range of measurement. Room temperature measurements of PSI isolated from higher plants show that for wavelengths shorter than 700 nm the emission is significantly weaker than that of PSII and it is characterised by an average decay lifetime of 20–40 ps (*e.g.* [28–39]). On the other hand, PSI shows

Abbreviations: PSI(II), Photosystem I (II); LHC, Light Harvesting Complex; Chl, chlorophyll; DAS, Decay Associated Spectra; F_0, fluorescence level at open PSII reaction centres; F_M, fluorescence level at closed PSII reaction centres; F_V, variable fluorescence; Φ_{PSII}^{max}, maximal photochemical yield of PSII; $\tau_{(av)}$, (average) lifetime; CP, chlorophyll protein complex

* Corresponding author at: Istituto di Biofisica, Consiglio Nazionale delle Ricerche, via Celoria 26, 20133 Milano, Italy. Tel.: +39 02 50314857.
E-mail address: stefano.santabarbara@cnr.it (S. Santabarbara).

http://dx.doi.org/10.1016/j.bbabio.2014.02.009
0005-2728/

a maximal fluorescence emission at about 720 nm, where PSII emission is minimal. Moreover the average excited state lifetime of isolated PSI increases in monotonic fashion up to 60–80 ps in the long wavelength range [28,34,37,38]. Thus PSI might be a source of error in the estimation of Φ_{PSII}^{max} if F_V/F_M is monitored at wavelengths above ~710–720 nm.

The use of the F_V/F_M ratio as an unbiased estimator of Φ_{PSII}^{max} also requires that this parameter is independent of both the excitation and the emission wavelength. This condition is attained if the band-shape of the PSII fluorescence emission spectrum is independent of both the excitation wavelength, and the active state of the reaction centre. Although it was shown that the emission spectrum of the isolated PSII–LHCII complex is substantially independent of excitation wavelength and, hence, that the system can be considered, to a good approximation, thermally equilibrated [40,41], it was also shown that the value of the F_V/F_M ratio (data were presented as F_0/F_M) is not constant through the emission spectrum [42–44]. Minimal values of F_0/F_M (corresponding to a maximal value of F_V/F_M) were observed in the 685–690 nm interval and interpreted in terms of an increase of photochemical quenching in the reaction centre complex, due to a partial kinetic bottleneck of excited state energy transfer from CP43 and CP47 [44,45]. This suggestion has been, in part, supported by kinetic modelling studies based on the crystallographic structures [46,47]. At the same time, spectroscopic studies performed either on the isolated core complex of PSII [48–52] or in PSII–LHCII complex [52–54], point towards a limited contribution of kinetic bottlenecks for energy transfer to the overall trapping kinetics.

Possible underestimations of the value of Φ_{PSII}^{max} obtained from F_V/F_M due to PSI emission have been already discussed in the literature (*e.g.* [15,53,55–57]). However, the dependence of Φ_{PSII}^{max} through the emission band has not been investigated under conditions in which PSII is embedded in its native membrane.

Therefore, we have performed a detailed *in vivo* investigation of both steady state and time resolved fluorescence emission under F_0 and F_M conditions in the green alga *Chlorella sorokiniana*. Both spectroscopic approaches demonstrate a pronounced variation of F_V/F_M across the emission band, with maximal values observed in the 660–680 nm interval and minimal values in the 700–720 nm window. The analysis of data indicates that PSI fluorescence emission is the principal cause of F_V/F_M spectral dependence, leading to an underestimation of the value of Φ_{PSII}^{max} between 5 and 20%, depending on the fluorescence detection wavelength.

2. Material and methods

2.1. Cell culture

C. sorokiana cells were grown under continuous illumination (80 μE m^{-2} s^{-1}) and shaking, at 25 °C in TAP medium, containing acetate as a carbon source. The culture was harvested during the logarithmic growth phase by centrifugation for 5 min at 1000 *g* and suspended in minimal media at an optical density of ~1 O.D. cm^{-1} at 680 nm. After 2 h of incubation under growth conditions, the cells were diluted to an optical density of 0.1 O.D. cm^{-1} in minimal medium supplemented with the non-osmotic polymer Ficoll (20% w/v) and further adapted for half an hour. The measurements were performed after a further 2 min of dark adaptation, for F_0 conditions. For measurements performed at F_M the PSII inhibitor DCMU (15 μM) was added to the dark-adapted sample.

2.2. Fluorescence emission spectroscopy

Fluorescence emission spectra were recorded using a laboratory assembled spectrometer using a liquid nitrogen cooled CCD camera (Princeton Applied Research, LN/CCD-ST138), coupled to a spectrograph (PAR, SpectraPro 300i) as a detector/analyser system, that has been described previously in detail [58]. The excitation source is a 250 W xenon lamp, filtered through a spectro-polarimeter (Jasco J500), a depolariser, a CS4-96 (Schott) band-pass filter and neutral density filters (Balzers) to control the excitation intensity. The excitation wavelength was set at 435 nm with a bandwidth of 1.5 nm, and it was sufficiently weak to maintain the cells in a state close to F_0, as judged from i) the F_V/F_M measured on the same sample after the addition of DCMU and ii) parallel measurements in a conventional fluorescence induction set-up. The spectra presented are the results of ten independent replicates (cell batches), each of which has been analysed three times on the same day of measurement. All spectra are corrected for the sensitivity of the detector, using a normalised instrument response function that maintains the experimental count number at the peak channel.

2.3. Measurement of the excited state lifetime

The decay of the excited state was monitored by the time-correlated single photon counting (TCSPC) technique in a home assembled set-up which has been previously described [34,52]. The excitation source was a diode laser (PicoQuant 800B) centred at 632 nm (FWHM 3 nm), with a pulse width of ~20 ps and operating at a repetition frequency of 20 MHz. The laser spot-size was about 1 mm in diameters and the pulse intensity is ~2 picoJ/pulse, which is sufficiently low to avoid the build-up of a significant population of closed centres at F_0 and of meta-stable states, such as (carotene) triplets. The emission was monitored at discrete wavelengths, selected by a monochromator (Jasco, JT-10), in the 660–750 nm interval. The detector was a cooled microchannel plate photomultiplier (Hamamatsu, R5916U-51). The overall response function of the instruments is 110 ± 10 ps, which allows resolving decay components which are an order of magnitude faster after numerical deconvolution. Measurements under F_0 and F_M conditions were performed on the same sample before and after DCMU was added. The sample was changed periodically during the measurement period. Moreover for each condition, measurements were performed by initially scanning from low to high wavelengths and subsequently in the reverse order. The instrument response function was determined using the dye DCI′ in ethanol as a reference standard, as previously described [52]. The results presented are the averages of eight independent cell batches.

2.4. Global analysis of TCSPC data

The kinetics of the excited state decay collected under F_0 and F_M conditions were analysed by iterative reconvolution of the instrument response and a sum of exponential functions, by a global fitting routine based on the MINUIT package that minimises the reduced χ^2 as previously described [52]. In brief the decay lifetimes (τ_i) are analysed as global parameters, whereas the pre-exponential amplitudes associated with each decay lifetime are treated as a local parameter and are therefore a function of the emission wavelength ($A_i(\lambda)$). The plot of the amplitude as a function of the emission wavelength yields the decay associated spectra (DAS). The quality of the fit was judged by the value of χ^2, inspection of the fit residuals and their autocorrelation and the band-shape of the DAS. It is a well known problem that such an analysis does not always lead to an unequivocal description of the data. As a rationale for selection amongst different possible fit solutions, we opted for those that were characterised by a minimal number of parameters and displayed stability through the independently tested cell batches.

The average lifetimes is defined as $\tau_{av} \equiv \left(\sum_{i=1}^{n} A_i \cdot \tau_i\right) / \sum_{i=1}^{n} A_i$.

3. Results and discussion

3.1. Steady state fluorescence emission spectra

The fluorescence emission spectra in whole cells of *C. sorokiniana*, under conditions in which the reaction centres of PSII are either open

(F_0) or closed (F_M), were initially studied under steady-state conditions. The cells were maintained at levels close to F_0, which is only attained for a dark-adapted system, and are thereafter referred to as F_0', by continuous illumination with a weak, monochromatic, excitation flux, (λ: 435 ± 1.5 nm equivalent to ~25 μE m^{-2} s^{-1}). The maximal fluorescence level, F_M, was obtained by the addition of the inhibitor DCMU (15 μM) under the same excitation conditions. The emission spectra collected at F_0' and F_M in several independent culture batches are presented in Fig. 1 (A). The emission spectrum at F_M represents the sum of the different independent acquisitions. In order to obtain the same signal-to-noise ratio at F_M and at F_0', a larger number of acquisitions (*i.e.* a factor of 4) were performed for the latter conditions maintaining constant the exposure time of each spectrum acquisition. The emission spectrum of F_0', shown in Fig. 1, was obtained as the sum of the acquired spectra, *scaled* for the numbers of acquisitions with respect to F_M. This procedure permits the difference in emission intensity to be maintained and to have spectra with similar statistical noise. To compare the changes in the emission band-shape of the spectra, recorded under conditions of open and closed reaction centres, these have been normalised to the respective emission maxima, which in both cases is 686 nm (Fig. 1B). In the main emission band, *i.e.* at wavelengths shorter than 700 nm, the normalised emission spectra recorded at F_0' and F_M substantially overlap. On the other hand, at wavelengths longer than 700 nm the normalised emission spectrum recorded under F_0' conditions is relatively more intense than that recorded under F_M conditions. This change in emission band-shape is further highlighted by calculating the difference ($F_0' - F_M$) of the normalised spectra (Fig. 1, insert), which shows two spectral features: i) a dominating feature, peaking at about 705 nm, which is relatively broad (about 25 nm at FWHM) and asymmetric and ii) a minor one, between 645 and 680 nm, which resembles a spectral structure that has been previously assigned to a small population of Chl–protein complexes in which some pigments are weakly coupled to the bulk antenna [59–61]. Since the difference spectra can be distorted, in part, by the choice of normalisation, and this might affect the assignment of the spectral features observed, we have also calculated the F_V'/F_M spectrum (with $F_V' = F_M - F_0'$), based on the measurements reported in Fig. 1A. The spectrum of F_V'/F_M presented in Fig. 2 does not rely on normalisation. Moreover, these F_V'/F_M values might be directly compared with those obtained by commonly employed steady-state methods which lack the spectral resolution of the present measurements. Fig. 2 shows that the value of F_V'/F_M has a significant emission wavelength dependence. Due to the large signal-to-noise ratio of the emission spectra the spectral dependence of F_V'/F_M is statistically significant, as indicated by the uncertainty bounds (Fig. 2). Maximal values in the range of 0.70–0.72 are observed in the 650–685 nm window, where the F_V'/F_M attains values close to those commonly reported by classic fluorescence "induction" techniques (*e.g.* [8–15]). We obtained values of about 0.75 by measurements of the induction curve in the presence of DCMU, upon excitation at 480 nm and detection at 680 nm (data not shown), that are comparable to the results presented in Fig. 2 calculated from the F_0' and F_M steady state emission spectra. In the F_V'/F_M spectrum minimal values of ~0.67 are observed at 710 nm, associated with a broad trough in the spectrum which extends from above 695 nm and up to 750 nm (Fig. 2). The band-shape of F_V'/F_M variation across the emission band appears to be associated principally with the contribution of PSI fluorescence to the total cell emission. PSI emission is expected to be very weakly dependent on the redox state of cofactors within the reaction centres [62,63] and independent from the active state of PSII. Still, based on the steady state measurements alone it is not possible to estimate possible contributions of PSI emission in the short wavelength (650–685 nm) window, which could also lead to an underestimation of the real value of PSII-associated F_V. The possible presence of a proper

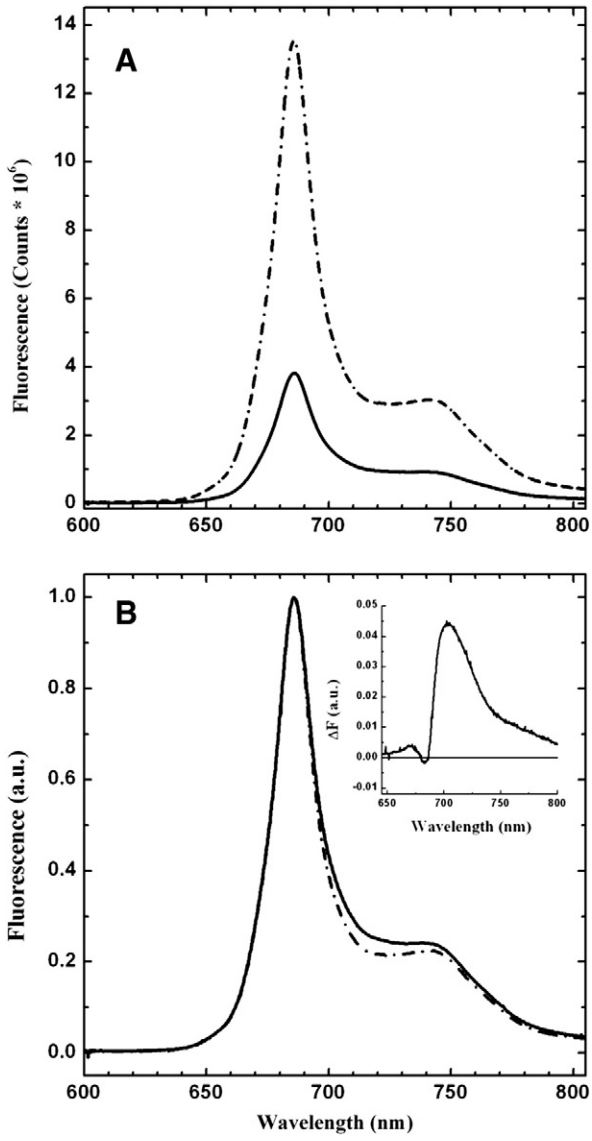

Fig. 1. Steady-state fluorescence emission spectra recorded under F_0' (continuous line) and F_M (dash-dotted line) conditions at room temperature (298 K). (A) Spectra scaled for the intensity of the emission, integrated over 8 independent cultures. (B) Spectra normalised at the emission maximum (686 nm). The insert of panel B shows the ($F_0' - F_M$) difference spectrum, after normalisation.

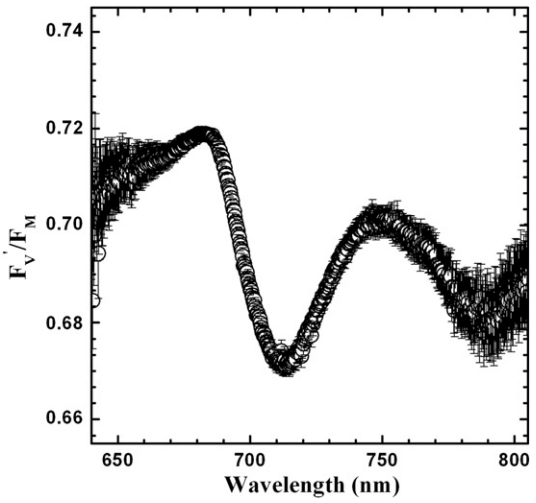

Fig. 2. Spectral dependence of the F_V'/F_M calculated from the spectra presented in Fig. 1A. The confidence bars are estimated after propagation of errors obtained according to Poisson statistics for the counts in each channel (wavelength) of the detector.

spectral dependence of photochemical quenching in PSII needs also to be considered. In order to get further information on these issues, the emission characteristics under F_0' and F_M conditions were investigated by monitoring the decay of the excited state with picosecond resolution.

3.2. Time-resolved fluorescence emission spectra

The results of the global analysis of the excited state kinetics under F_0' and F_M conditions, presented as the average of several independent measurements on different algal batches, are shown in Fig. 3. The amplitude of the decay associated spectra (DAS = $A_i(\lambda)$) are scaled in order to maintain the difference in the intensity of the fluorescence emission at F_0' and F_M, that is given by the integrated count number under the TCSPC traces. This scaling is possible because the measurements at open and closed reaction centres were performed on the same samples.

Under F_0' conditions the data are described satisfactorily considering five exponential components, characterised by the following lifetimes: 53 ± 7 ps, 89 ± 9 ps, 174 ± 23 ps, 535 ± 67 ps and 1.2 ± 0.2 ns.

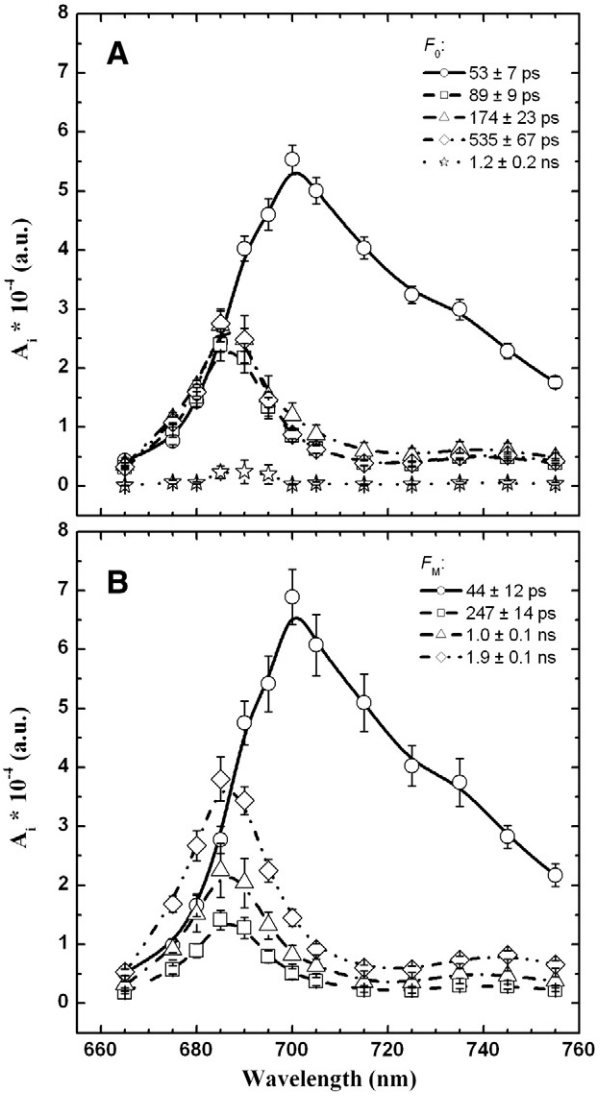

Fig. 3. Decay associated spectra (DAS) obtained from the global analysis of TCSPC data, under F_0' (A) and F_M (B) conditions. Panel A, F_0': 53 ± 7 ps, circles/solid line; 89 ± 9 ps, squares/dashed line; 174 ± 23 ps, triangles, dash-dotted line; 535 ± 67 ps, diamonds/dash-dot-dotted line, 1.2 ± 0.1 ns, stars/dotted line. Panel B, F_M: 44 ± 12 ps, circles/solid line; 247 ± 14 ps, squares/dashed line; 1.0 ± 0.1 ns, triangles/dash-dotted line; 1.9 ± 0.1 ns, diamonds/dash-dot-dotted line. The confidence levels are the standard deviation associated with the weighted mean.

These values fall in the range of the relatively broad distribution of the decay lifetimes reported in the literature for time-resolved fluorescence studies in thylakoids, leaves and algal cells of different species (*e.g.* [20–25]). The lifetimes in the 80–550 ps interval display very similar DAS band-shape, with maxima close to 685 nm and relatively weak amplitude above 700 nm. On the other hand, the DAS associated with the shortest 53 ± 7 ps component are maximal above 700 nm.

Under F_M conditions four exponential components are sufficient to describe satisfactorily the excited state decay. These are characterised by lifetimes of 44 ± 12 ps, 274 ± 14 ps, 1.0 ± 0.1 ns and 1.9 ± 0.1 ns. Under F_M conditions the DAS associated with lifetimes in the 270 ps–2 ns interval have similar band-shape, maximal values at 685 nm and show a weak tail above 700 nm, similar to that observed for components in the 80–550 ps interval at F_0' but for the increase in lifetimes. Both the lifetime and the DAS of the fastest component (44 ± 12 ps at F_M) do not change significantly when PSII centres are open or closed. Fig. 4 shows a direct comparison of the integrated emission ($A(\lambda) \cdot \tau$) associated with the fastest decay component derived from the F_0' and F_M analysis. Since no further scaling or normalisation has been applied other than that described for the data presented in Fig. 3, it can be concluded that the contribution of the fastest decay lifetime to the total fluorescence emission is independent on the photochemical state of PSII. This evidence, together with the red-shifted emission with respect to all other DAS, leads us to the assignment of the 30–50 ps decay to PSI. The description of PSI emission in terms of a single exponential is probably a simplification on the basis of measurements obtained in isolated systems (*e.g.* [28–39]). However, increasing the number of exponential components in the fit did not yield either better statistics, in terms of reducing χ^2, or additional DAS components which could be related to specific PSI decays (*i.e.* red emission forms of PSI). We notice that the DAS associated with the 30–50 ps decay, although red-shifted with respect to the other DAS in *C. sorokiniana*, are markedly blue shifted with respect to PSI of higher plants (*e.g.* [25,28,35–39]), where the long wavelength emission forms are associated with LHCI (*e.g.* [64–68]). This indicates a difference in the PSI antenna characteristic in green algae, in agreement with the observation obtained comparing both the low temperature (77 K and below) fluorescence emission spectra of green algae (*e.g.* [69–71]) and higher plants thylakoid (*e.g.* [10,72,73]), as well as from study of isolated [74] and reconstituted [75] LHCI complexes from another model alga, *C. reinhardtii*. The main reason for a multi-exponential decay in PSI

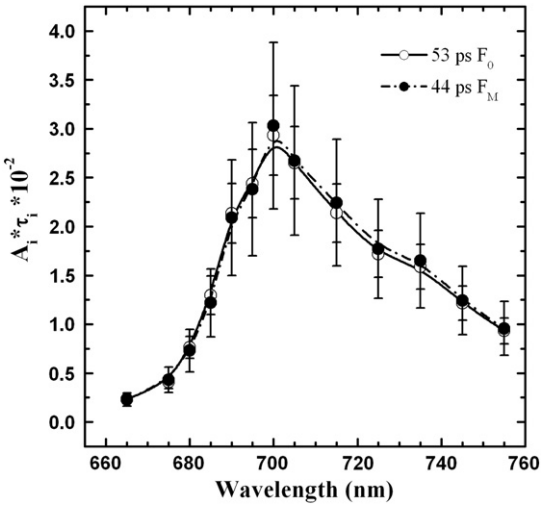

Fig. 4. Comparison of the reconstructed steady-state spectra ($F_{SS} = A(\lambda) \cdot \tau$) associated with the faster decay component detected at F_0' (τ = 53 ± 7, open circles/solid line) and F_M (τ = 44 ± 12 ps, closed circle/dash-dotted line). The confidence levels are the propagation of the standard deviations associated to $A(\lambda)$ and τ.

of higher plants has been related to the presence of kinetic bottlenecks for energy transfer due to the presence of red-forms in the antenna (*e.g.* [34,36–39,76]). A lower abundance of these pigments and/or a less pronounced spectral dispersion might lead to a simplification of the excited state dynamics in the PSI of *C. sorokiniana* compared to that of higher plants. Thus, to a first order approximation, it would seem possible to consider the ~45 ps lifetime observed *in vivo* as a macroscopic description of the excited state decay in PSI, that approximates the *overall* (photosystem-level) average lifetime determined in several studies on isolated PSI (*e.g.* [28–39]).

The other DAS are then assigned to PSII on the basis of the band-shape and the increase in the value of τ when the PSII reaction centre is closed. To further confirm this assignment, the reconstruction of the steady state spectra calculated as $F_{SS} = \sum_{i=1}^{n} A_i(\lambda) \cdot \tau_i$, considering the 89 ± 9 ps, 174 ± 23 ps, 535 ± 67 ps at F_0' and 274 ± 14 ps, 1.0 ± 0.1 ns and 1.9 ± 0.1 ns at F_M, is presented in Fig. 5A. The longest lifetime of ~1.2 ns observed under F_0' conditions has a very small amplitude at all detected wavelengths (<3%) and the value of this τ approaches that of τ_{av} measured under F_M conditions. Hence, also in accordance with several other studies (*e.g.* [18–28]), we consider this lifetime to describe a small population of PSII centres which are closed under our F_0' measurement conditions and that are described macroscopically by a single decay lifetime. This lifetime has therefore been excluded from this analysis. In Fig. 5B the same spectra are normalised to the maximal emission and compared to the (normalised) spectrum of variable fluorescence, obtained from the steady-state measurements of Fig. 1. The comparison shows that there is little variation in the band-shape of the emission spectra under F_0' and F_M conditions, and that both DAS-derived spectra overlap almost perfectly to that of F_V' obtained in the steady-state, which then represents the *in vivo* PSII emission spectrum.

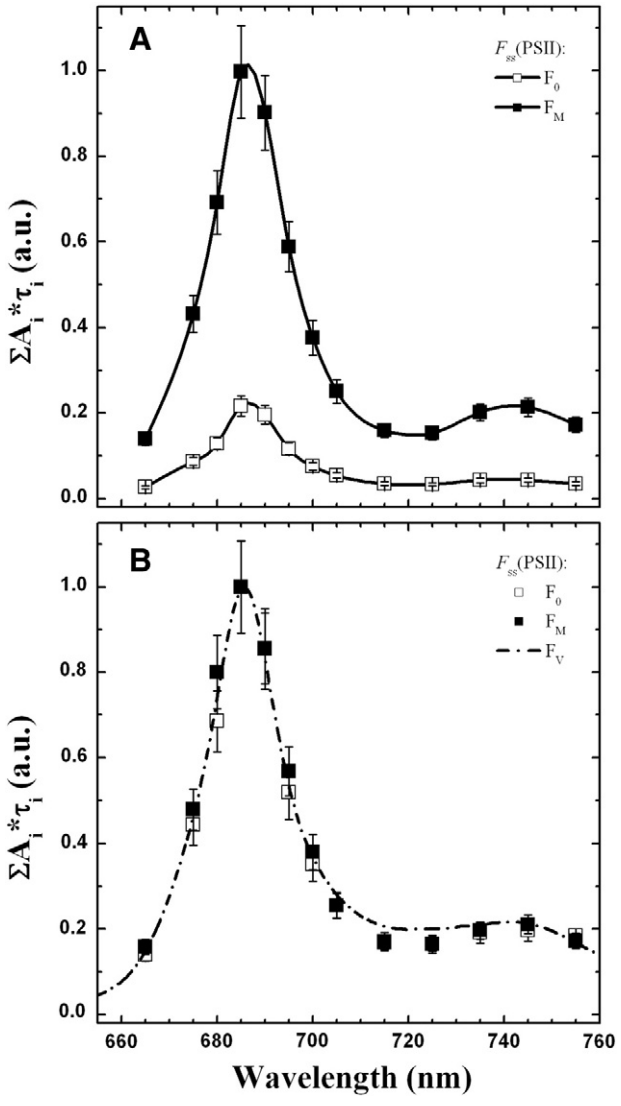

Fig. 5. Comparison of the reconstructed steady-state spectra of PSII ($F_{SS,PSII} = Ai(\lambda) \cdot \tau_i$ at F_0' (τ_i = 89 ± 9 ps, 174 ± 23 ps and 535 ± 67 ps components, open circles/solid line) and F_M (τ_i = 247 ± 14 ps, 1.0 ± 0.1 ns and 1.9 ± 0.1 ns, closed circle/dash-dotted line). (A) Intensity-scaled reconstruction of $F_{SS,0}$ (PSII) and $F_{SS,0}$ (PSII). (B) Spectra of Panel A normalised to the maximal emission (685 nm) and compared with the normalised (at the maximum) F_V spectrum (dash-dotted line) obtained from the difference of the spectra at F_M and F_0' shown in Fig. 1A. The confidence levels are the propagation of the standard deviations associated with $A_i(\lambda)$ and τ_i.

Having assigned the lifetime components associated with the emission of both PSI and PSII, both under F_0' and F_M conditions, it is possible to evaluate the relative contribution of the two photosystems to the total emission and their impact in the determination of the F_V'/F_M ratio. The calculations were performed by reconstructing the steady-state levels (F_{SS}) starting from the time resolved data (Fig. 6). When all the measured decay components are considered F_V'/F_M has maximal values in the 670–680 nm range ($F_V'/F_M = 0.78$), whereas a decrease of the ratio, with a minima at 710 nm ($F_V'/F_M = 0.67$) is observed on the long wavelength tail of the emission. Neglecting the contribution of the 1.2 ns component detected at F_0' from the calculations, since this was attributed to small population of closed centres, yields larger values of F_V/F_M across the entire emission band, but does not alter significantly the wavelength dependence of the parameter. On the other hand, when the long-lived 1.2 ns component was omitted at F_0' *and* the faster lifetimes, attributed to PSI, were omitted both at F_0' and F_M, the F_V'/F_M ratio attains its maximal value (around 0.80) and the spectral dependence becomes significantly weaker, with a minima of ~0.78 observed in the 685–690 nm interval.

3.3. Factors influencing the estimation of maximal photochemical efficiency of PSII (Φ_{PSII}^{max}) from the F_V/F_M ratio

The measurement of the F_V/F_M ratio has become a widespread technique to estimate Φ_{PSII}^{max} and its variation under various environmental and experimental conditions (*e.g.* [13,15]). One of the principal advantages of the so-called fluorescence induction technique is that it can be performed *in vivo*, *i.e.* with leaves or cell suspensions, so that the samples are closely related to physiological conditions and perturbations

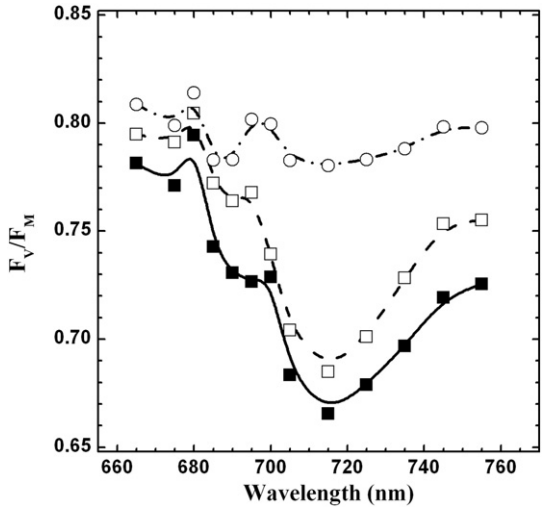

Fig. 6. Calculations of F_V'/F_M from the reconstructed steady state spectra, F_{SS} obtained from the global analysis of the excited state decay at F_0' and F_M. (A) Solid squares/solid line: F_V'/F_M ratio considering all the measured lifetime; open squares/dashed line: excluding the 1.2 ± 0.1 ns component from the reconstruction of $F_{SS,0}$; open circles/dash-dotted line: excluding the 1.2 ± 0.1 ns and the 53 ± 7 components from the reconstruction of $F_{SS,0}$ and the 44 ± 12 ps from the reconstruction of $F_{SS,M}$ lines.

due to the absence of biochemical purification. These measurements are most commonly performed at a single excitation/detection wavelength, be it narrow or broadband. This approach relies on the assumption that the photochemical yield of PSII is independent on the detection/excitation wavelength and that the emission of PSI, at room temperature, is negligible. The reinvestigation of the emission wavelength dependence of the F_V/F_M ratio in whole cells of *C. sorokiniana* demonstrates, instead, that there is a significant variation of this parameter across the emission band (Figs. 2 and 6). Maximal values are observed in the short emission wavelength range, close to the emission maximum, whereas minimal values are observed in the 700–720 nm interval. The shape of the spectral dependence of the F_V/F_M ratio and the analysis of excited state relaxation under F_0' and F_M conditions indicate that the principal source of spectral distortion in the estimation of Φ_{PSII}^{max} is due to PSI emission, whereas the condition that PSII quantum yield is constant through the emission band is substantially verified.

The spectral dependence of F_V/F_M is explainable in simple terms by describing the emission at F_0' and F_M as a linear combination of PSI and PSII emission spectra:

$$\begin{cases} F_0'(\lambda) = \phi_{II,0} \cdot f_{II}(\lambda) + \phi_I \cdot f_I(\lambda) \cdot \\ F_M(\lambda) = \phi_{II,M} \cdot f_{II}(\lambda) + \phi_I \cdot f_I(\lambda) \end{cases} \quad (1)$$

where $f_{II}(\lambda)$ and $f_i(\lambda)$ are the band-shapes of PSII and PSI emissions, respectively, $\phi_{II,0}$ and $\phi_{II,M}$ are the fluorescence yields of PSII when the centres are open and closed, respectively, and ϕ_I is the yield of PSI fluorescence. This expression is based on the time-resolved measurements indicating that the emission of PSI ($\phi_I \cdot f_I(\lambda)$) remains unchanged under the measuring F_0' and F_M conditions (Fig. 4), and that the band-shape of PSII ($f_{II}(\lambda)$) does not change significantly when PSII RC are either open or closed (Fig. 5).

With these assumptions, $F_V(\lambda) = (\phi_{II,M} - \phi_{II,0}) \cdot f_{II}(\lambda)$ and the spectral dependence of F_V/F_M becomes:

$$\frac{F_V}{F_M}(\lambda) = \frac{\left(\phi_{II,M} - \phi_{II,0}\right) \cdot f_{II}(\lambda)}{\phi_{II,M} \cdot f_{II}(\lambda) + \phi_I \cdot f_I(\lambda)}. \quad (2)$$

From Eq. (2) it is apparent that F_V/F_M reaches its maximal value when $f_I(\lambda)$, *i.e.* the band-shape of PSI emission spectrum, reaches its minimum, and *vice-versa*, as observed in the measurements (Figs. 2 and 6). Thus, PSI emission can lead to an underestimation of Φ_{PSII}^{max} by up to 20% in the 700–720 nm range, and of 2–5% even at shorter wavelengths where PSII emission is dominant. The degree of spectral distortion of Φ_{PSII}^{max} will obviously depend on the PSI emission characteristics in difference species, and the value retrieved in this study should be considered accurate only for the organism investigated, or, at best, for green algae. Yet, although the extent of such spectral distortion could be variable, the phenomena discussed should be common to all oxygenic organisms possessing a Chl *a*/*b*-binding external antenna.

3.4. Wavelength-dependence of the photochemical quantum yield in PSII

Another factor that could potentially contribute to the wavelength dependence of the F_V/F_M ratio is the variation of the *effective* trapping time across the emission band of PSII. The spectral dependence of photochemical quenching, giving rise to a maximal value of F_V/F_M at about 690 nm, has been previously reported in experiments performed on isolated thylakoids and PSII particles (BBY membrane) [42–44]. As distinct from the case of spectral distortion due to PSI emission, this would represent a proper wavelength dependence of Φ_{PSII}^{max}, that was interpreted as resulting from kinetic bottlenecks for energy transfer from the core antenna complexes to the reaction centre [44–47].

It has been previously demonstrated for a photochemically active centre, such as PSII under F_0' conditions, that τ_{av} represents a good estimate of the *effective* photochemical trapping time [76]. Hence, to investigate the spectral dependence of PSII photochemical trapping *in vivo*, the wavelength dependence of τ_{av} has been computed (eliminating the faster decay component that was attributed to PSI). Fig. 7A shows the spectral dependence of $\tau_{av,0}$, that is calculated from the data obtained under F_0' conditions ($\tau_{av,0}$). The wavelength dependence of τ_{av} calculated at F_M ($\tau_{av,M}$) is also shown for comparison (Fig. 7B). The wavelength dependence of $\tau_{av,M}$ appears to be relatively constant through the emission band, with minor, scattered, variations.

On the other hand, the spectral dependence of $\tau_{av.0}$ is more pronounced. The values of $\tau_{av.0}$ across the entire band appear to fall in between the estimates of the same parameters obtained in isolated BBY membranes, which are in the 150–200 ps interval (*e.g.* [26–28,53,54]), and those obtained in isolated thylakoids which were reported to be in the range of 350–400 ps (*e.g.* [20,25]). While it is evident that when the single points are considered, the large error bars may suggest that significant differences across the emission band do not exist, one should however note that the spectral variation across the emission band is maintained when considering the lower and upper statistical significance bounds. The minimal values of $\tau_{av.0}$ ~ 255 ps, corresponding to the maximal photochemical quenching, are obtained in the 695–710 nm

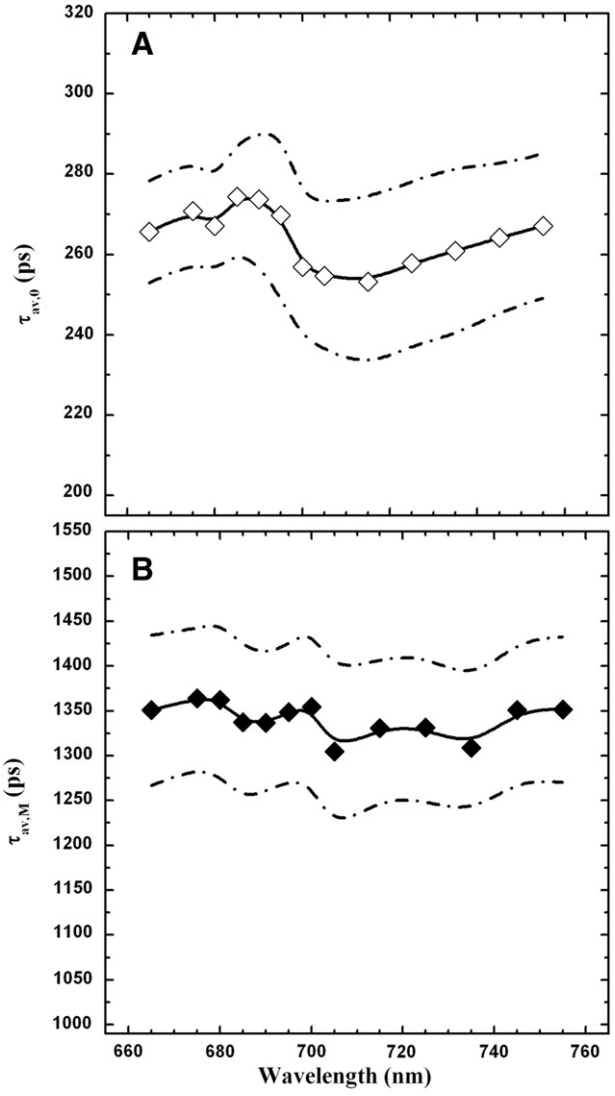

Fig. 7. Spectral dependence of $\tau_{av,0}$ (A) and $\tau_{av,M}$ (B) associated with PSII. $\tau_{av,0}$ was computed considering the 89 ± 9 ps, 174 ± 23 ps and 535 ± 67 ps components and $\tau_{av,M}$ considering the 247 ± 14 ps, 1.0 ± 0.1 ns and 1.9 ± 0.1 ns components. The continued dash–dotted lines mark the upper and lower confidence levels determined from the propagation of the standard deviations associated with $A_i(\lambda)$ and τ_i.

range, *i.e.* are red-shifted with the respect to the maximal emission. This observation is in substantial agreement with previous results obtained with isolated PSII, where maximal quenching was detected at 690 nm [42–44], by steady-state methods. The results were interpreted as being due to fast photochemistry leading to a selective quenching of the core complex [44]. Similar conclusions were later obtained also by time-resolved fluorescence analysis of the BBY membranes [54]. It is not unreasonable to suggest that the present spectral variation in τ_{av} is due to a similar phenomenon. However, we underline that the overall variation of $\tau_{av,0}$ across the band is only about 20 ps with respect to an overall mean value of 265 ps, *i.e.* less than 8%. Therefore, in terms of Φ_{PSII}^{max} estimation this effect is moderate.

References

[1] R. Kouril, J.P. Dekker, E.J. Boekema, Supramolecular organization of photosystem II in green plants, Biochim. Biophys. Acta Bioenerg. 1817 (2012) 2–12.
[2] A. Guskov, J. Kern, A. Gabdulkhakov, M. Broser, A. Zouni, W. Saenger, Cyanobacterial photosystem II at 2.9-Å resolution and the role of quinones, lipids, channels and chloride, Nat. Struct. Mol. Biol. 16 (2009) 334–342.
[3] S. Caffarri, R. Kouril, S. Kereiche, E.J. Boekema, R. Croce, Functional architecture of higher plant photosystem II supercomplexes, EMBO J. 2 (2009) 3052–3063.
[4] Y. Umena, K. Kawakami, J.R. Shen, N. Kamiya, Crystal structure of oxygen-evolving photosystem II at a resolution of 1.9 Å, Nature 473 (2011) 55–60.
[5] S. Jansson, The light-harvesting chlorophyll a/b-binding proteins, Biochim. Biophys. Acta Bioenerg. 1184 (1994) 1–19.
[6] R.C. Jennings, R. Bassi, G. Zucchelli, Antenna structure and energy transfer in higher plant photosystems, Topics in Current Chemistry, Electron Transfer II, vol.177, Springer, Berlin, 1996, pp. 147–181.
[7] D. Sandonà, R. Croce, A. Pagano, M. Crimi, R. Bassi, Higher plants light harvesting proteins. Structure and function as revealed by mutation analysis of either protein or chromophore moieties, Biochim. Biophys. Acta Bioenerg. 1365 (1998) 207–214.
[8] P. Joliot, A. Joliot, Etudes cinétique de la réaction photochimique libérant l'oxygene au cours de la photosynthese, C. R. Acad. Sci. Paris 258 (1964) 4622–4625.
[9] G. Paillotin, Capture frequency of excitations and energy transfer between photosynthetic units in the photosystem II, J. Theor. Biol. 58 (1976) 219–235.
[10] W.L. Butler, Energy distribution in the photochemical apparatus of photosynthesis, Annu. Rev. Plant Physiol. Plant Mol. Biol. 29 (1978) 345–378.
[11] L.N. Duysens, Transfer and trapping of excitation energy in photosystem II, Ciba Found. Symp (1978) 323–340.
[12] H.J. Van Gorkom, Electron transfer in Photosystem II, Photosynth. Res. 6 (1985) 97–112.
[13] J. Lavergne, H.W. Trissl, Theory of fluorescence induction in Photosystem II: derivation of analytical expressions in a model including exciton–radical-pair equilibrium and restricted energy transfer between photosynthetic units, Biophys. J. 68 (1995) 2474–2492.
[14] G.H. Krause, E. Weis, Chlorophyll fluorescence and photosynthesis: the basics, Annu. Rev. Plant Physiol. Plant Mol. Biol. 31 (1991) 202–238.
[15] N.R. Baker, Chlorophyll fluorescence: a probe of photosynthesis *in vivo*, Annu. Rev. Plant Biol. 59 (2008) 89–113.
[16] G.F. Searle, C.J. Tredwell, J. Barber, G. Porter, Picosecond time-resolved fluorescence study of chlorophyll organisation and excitation energy distribution in chloroplasts from wild-type barley and a mutant lacking chlorophyll b, Biochim. Biophys. Acta Bioenerg. 545 (1979) 496–507.
[17] K.K. Karukstis, K. Sauer, The effects of cation-induced and pH-induced membrane stacking on chlorophyll fluorescence decay kinetics, Biochim. Biophys. Acta 806 (1985) 374–388.
[18] A.R. Holzwarth, J. Wendler, W. Haehnel, Time-resolved picosecond fluorescence spectra of the antenna chlorophylls in *Chlorella vulgaris*. Resolution of photosystem I fluorescence, Biochim. Biophys. Acta Bioenerg. 807 (1985) 155–167.
[19] K.K. Karukstis, K. Sauer, Picosecond fluorescence studies of electron acceptor Q redox heterogeneity, Biochim. Biophys. Acta 725 (1983) 246–253.
[20] M. Hodges, I. Moya, Time-resolved chlorophyll fluorescence studies of photosynthetic membranes: resolution and characterization of four kinetic components, Biochim. Biophys. Acta Bioenerg. 849 (1986) 193–202.
[21] I. Moya, M. Hodges, J.-M. Briantais, G. Hervo, Evidence that the variable chlorophyll fluorescence in *Chlamydomonas reinhardtii* is not recombinant luminescence, Photosynth. Res. 10 (1986) 319–325.
[22] T.A. Roelofs, C.H. Lee, A.R. Holzwarth, Global target analysis of picosecond chlorophyll fluorescence kinetics from pea chloroplasts. A new approach to the characterization of the primary processes in photosystem II alfa- and beta-units, Biophys. J. 61 (1992) 1147–1163.
[23] J.M. Briantais, J. Dacosta, Y. Goulas, J.M. Ducruet, I. Moya, Heat stress induces in leaves an increase of the minimum level of chlorophyll fluorescence, F_0: a time-resolved analysis, Photosynth. Res. 48 (1996) 189–196.
[24] A.M. Gilmore, V.P. Shinkarev, T.L. Hazlett, G. Govindjee, Quantitative analysis of the effects of intrathylakoid pH and xanthophyll cycle pigments on chlorophyll a fluorescence lifetime distributions and intensity in thylakoids, Biochemistry 37 (1998) 13582–13593.
[25] E.C.M. Engelmann, G. Zucchelli, F.M. Garlaschi, A.P. Casazza, R.C. Jennings, The effect of outer antenna complexes on the photochemical trapping rate in barley thylakoid Photosystem II, Biochim. Biophys. Acta Bioenerg. 1706 (2005) 276–286.
[26] K. Broess, G. Trinkunas, A. van Hoek, R. Croce, H. van Amerongen, Determination of the excitation migration time in Photosystem II consequences for the membrane organization and charge separation parameters, Biochim. Biophys. Acta 1777 (2008) 404–409.
[27] B. van Oort, M. Alberts, S. de Bianchi, L. Dall'Osto, R. Bassi, G. Trinkunas, R. Croce, H. van Amerongen, Effect of antenna-depletion in Photosystem II on excitation energy transfer in *Arabidopsis thaliana*, Biophys. J. 98 (2010) 922–931.
[28] R. Croce, D. Dorra, A.R. Holzwarth, R.C. Jennings, Fluorescence decay and spectral evolution in intact photosystem I of higher plants, Biochemistry 39 (2000) 6341–6348.
[29] B. Gobets, R. van Grondelle, Energy transfer and trapping in Photosystem I, Biochim. Biophys. Acta Bioenerg. 1057 (2001) 80–99.
[30] J.A. Ihalainen, P.E. Jensen, A. Haldrup, I.H.M. van Stokkum, R. van Grondelle, H.V. Scheller, J.P. Dekker, Pigment organization and energy transfer dynamics in isolated, photosystem I (PSI) complexes from *Arabidopsis thaliana* depleted of the PSI-G, PSI-K, PSI-L, or PSI-N subunit, Biophys. J. 83 (2002) 2190–2201.
[31] J.A. Ihalainen, F. Klimmek, U. Ganeteg, I.H.M. van Stokkum, R. van Grondelle, S. Jansson, J.P. Dekker, Excitation energy trapping in photosystem I complexes depleted in Lhca1 and Lhca4, FEBS Lett. 579 (2005) 4787–4791.
[32] J.A. Ihalainen, I.H.M. van Stokkum, K. Gibasiewicz, M. Germano, R. van Grondelle, J.P. Dekker, Kinetics of excitation trapping in intact Photosystem I of *Chlamydomonas reinhardtii* and *Arabidopsis thaliana*, Biochim. Biophys. Acta Bioenerg. 1706 (2005) 267–275.
[33] A.R. Holzwarth, M.G. Muller, J. Niklas, W. Lubitz, Charge recombination fluorescence in photosystem I reaction centers from *Chlamydomonas reinhardtii*, J. Phys. Chem. B 109 (2005) 5903–5911.
[34] E. Engelmann, G. Zucchelli, A.P. Casazza, D. Brogioli, F.M. Garlaschi, R.C. Jennings, Influence of the photosystem I-light harvesting complex I antenna domains on fluorescence decay, Biochemistry 45 (2006) 6947–6955.
[35] C. Slavov, M. Ballottari, T. Morosinotto, R. Bassi, A.R. Holzwarth, Trap-limited charge separation kinetics in higher plant photosystem I complexes, Biophys. J. 94 (2008) 3601–3612.
[36] E. Wientjes, I.H. van Stokkum, H. van Amerongen, R. Croce, The role of the individual Lhcas in photosystem I excitation energy trapping, Biophys. J. 101 (2011) 745–754.
[37] P. Galka, S. Santabarbara, T.T. Khuong, H. Degand, P. Morsomme, R.C. Jennings, E.J. Boekema, S. Caffarri, Functional analyses of the plant photosystem I-light-harvesting complex II supercomplex reveal that light-harvesting complex II loosely bound to photosystem II is a very efficient antenna for photosystem I in state II, Plant Cell 24 (2012) 2963–2978.
[38] R.C. Jennings, G. Zucchelli, S. Santabarbara, Photochemical trapping heterogeneity as a function of wavelength, in plant photosystem I (PSI-LHCI), Biochim. Biophys. Acta Bioenerg. 1827 (2013) 779–785.
[39] E. Wientjes, H. van Amerongen, R. Croce, LHCII is an antenna of both photosystems after long-term acclimation, Biochim. Biophys. Acta Bioenerg. 1827 (2013) 420–426.
[40] R.C. Jennings, R. Bassi, F.M. Garlaschi, P. Dainese, G. Zucchelli, Distribution of the chlorophyll spectral forms in the chlorophyll/protein complexes of Photosystem-II antenna, Biochemistry 32 (1993) 3203–3210.
[41] H. Dau, K. Sauer, Exciton equilibration and photosystem II exciton dynamics. A fluorescence study on photosystem II membrane particles of spinach, Biochim. Biophys. Acta Bioenerg. 1273 (1996) 175–190.
[42] R.C. Jennings, G. Zucchelli, F.M. Garlaschi, The influence of quenching by open reaction centres on the photosystem II fluorescence emission spectrum, Biochim. Biophys. Acta Bioenerg. 1060 (1991) 245–250.
[43] R.C. Jennings, G. Zucchelli, F.M. Garlaschi, A. Vianelli, A comparison of the light-induced, non-reversible, fluorescence quenching in photosystem II with quenching due to open reaction centres in terms of the chlorophyll emission spectral forms, Biochim. Biophys. Acta Bioenerg. 1101 (1992) 79–83.
[44] R.C. Jennings, G. Elli, F.M. Garlaschi, S. Santabarbara, G. Zucchelli, Selective quenching of the fluorescence of core chlorophyll-protein complexes by photochemistry indicates that Photosystem II is partly diffusion limited, Photosynth. Res. 66 (2000) 225–233.
[45] J.P. Dekker, R. Van Grondelle, Primary charge separation in Photosystem II, Photosynth. Res. 63 (2000) 195–208.
[46] S. Vasil'ev, P. Orth, A. Zouni, T.G. Owens, D. Bruce, Excited-state dynamics in photosystem II: insights from the X-ray crystal structure, Proc. Natl. Acad. Sci. U. S. A. 98 (2001) 8602–8607.
[47] G. Raszewski, T. Renger, Light harvesting in photosystem II core complexes is limited by the transfer to the trap: can the core complex turn into a photoprotective mode? J. Am. Chem. Soc. 130 (2008) 4431–4446.
[48] G.H. Schatz, H. Brock, A.R. Holzwarth, A kinetic and energetic model for the primary processes in photosystem II, Biophys. J. 54 (1988) 397–405.
[49] Y. Miloslavina, M. Szczepaniak, M.G. Muller, J. Sander, M. Nowaczyk, M. Rogner, A.R. Holzwarth, Charge separation kinetics in intact photosystem II core particles is trap-limited. A picosecond fluorescence study, Biochemistry 45 (2006) 2436–2442.
[50] M. Szczepaniak, J. Sander, M. Nowaczyk, M.G. Muller, M. Rogner, A.R. Holzwarth, Charge separation, stabilization, and protein relaxation in photosystem II core particles with closed reaction center, Biophys. J. 96 (2009) 621–631.
[51] A.R. Holzwarth, M.G. Muller, M. Reus, M. Nowaczyk, J. Sander, M. Rogner, Kinetics and mechanism of electron transfer in intact photosystem II and in the isolated reaction center: pheophytin is the primary electron acceptor, Proc. Natl. Acad. Sci. U. S. A. 103 (2006) 6895–6900.
[52] G. Tumino, A.P. Casazza, E. Engelmann, F.M. Garlaschi, G. Zucchelli, R.C. Jennings, Fluorescence lifetime spectrum of the plant photosystem II core complex: photochemistry does not induce specific reaction center quenching, Biochemistry 47 (2008) 10449–10457.

[53] S. Caffarri, K. Broess, R. Croce, H. van Amerongen, Excitation energy transfer and trapping in higher plant photosystem II complexes with different antenna sizes, Biophys. J. 100 (2011) 2094–2103.
[54] K. Broess, G. Trinkunas, C.D. van der Weij-de Wit, J.P. Dekker, A. van Hoek, H. van Amerongen, Excitation energy transfer and charge separation in photosystem II membranes revisited, Biophys. J. 91 (2006) 3776–3786.
[55] M. Stroch, J. Podolinsa, M. Navratil, V. Spunda, Effects of different excitation and detection spectral regions on room temperature chlorophyll a fluorescence parameters, Photosynthetica 43 (2005) 411–416.
[56] E.E. Pfündel, Deriving room temperature excitation spectra for photosystem I and photosystem II fluorescence in intact leaves from the dependence of F_V/F_M on excitation wavelength, Photosynth. Res. 100 (2009) 163–167.
[57] E.E. Pfündel, C. Klughammer, A. Meister, Z.G. Cerovic, Deriving fluorometer-specific values of relative PSI fluorescence intensity from quenching of F_0 fluorescence in leaves of *Arabidopsis thaliana* and *Zea mays*, Photosynth. Res. 114 (2013) 189–206.
[58] R.C. Jennings, G. Zucchelli, E. Engelmann, F.M. Garlaschi, The long-wavelength chlorophyll states of plant LHCI at room temperature: a comparison with PSI-LHCI, Biophys. J. 87 (2004) 488–497.
[59] S. Santabarbara, K.V. Neverov, F.M. Garlaschi, G. Zucchelli, R.C. Jennings, Involvement of uncoupled antenna chlorophylls in photoinhibition in thylakoids, FEBS Lett. 491 (2001) 109–113.
[60] S. Santabarbara, I. Cazzalini, A. Rivadossi, F.M. Garlaschi, G. Zucchelli, R.C. Jennings, Photoinhibition *in vivo* and *in vitro* involves weakly coupled chlorophyll-protein complexes, Photochem. Photobiol. 75 (2002) 613–618.
[61] S. Santabarbara, R.C. Jennings, The size of the population of weakly coupled chlorophyll pigments involved in thylakoid photoinhibition determined by steady-state fluorescence spectroscopy, Biochim. Biophys. Acta Bioenerg. 1709 (2005) 138–149.
[62] M. Byrdin, I. Rimke, E. Schlodder, D. Stehlik, T.A. Roelofs, Decay kinetics and quantum yields of fluorescence in photosystem I from *Synechococcus elongatus* with P700 in the reduced and oxidized state: are the kinetics of excited state decay trap-limited or transfer-limited? Biophys. J. 79 (2000) 992–1007.
[63] N.T.G. White, G.S. Beddard, J.R.G. Thorne, T.M. Feehan, T.E. Keyes, Primary charge separation and energy transfer in Photosystem I reaction centre of higher plants, J. Phys. Chem. B 100 (1996) 12086–12099.
[64] R. Croce, G. Zucchelli, F.M. Garlaschi, R.C. Jennings, Excited state equilibration in the photosystem I-light-harvesting I complex: P700 is almost isoenergetic with its antenna, Biochemistry 35 (1996) 8572–8579.
[65] R. Croce, G. Zucchelli, F.M. Garlaschi, R.C. Jennings, A thermal broadening study of the antenna chlorophylls in PSI-200, LHCI, and PSI core, Biochemistry 37 (1998) 17355–17360.
[66] R. Croce, T. Morosinotto, S. Castelletti, J. Breton, R. Bassi, The Lhca antenna complexes of higher plants photosystem I, Biochim. Biophys. Acta Bioenerg. 1556 (2002) 29–40.
[67] R.C. Jennings, F.M. Garlaschi, E. Engelmann, G. Zucchelli, The room temperature emission band shape of the lowest energy chlorophyll spectral form of LHCI, FEBS Lett. 547 (2003) 107–110.
[68] E. Wientjes, R. Croce, The light-harvesting complexes of higher-plant Photosystem I: Lhca1/4 and Lhca2/3 form two red-emitting heterodimers, Biochem. J. 433 (2011) 477–485.
[69] F. Cho, Govindjee, Fluorescence spectra of *Chlorella* in the 295–77°K range, Biochim. Biophys. Acta Bioenerg. 205 (1970) 371–378.
[70] F. Cho, Govindjee, Low-temperature (4–77°K) spectroscopy of *Chlorella*; temperature dependence of energy transfer efficiency, Biochim. Biophys. Acta Bioenerg. 216 (1970) 139–150.
[71] S. Santabarbara, G. Agostini, A.P. Casazza, C.D. Syme, P. Heathcote, F. Böhles, M.C.W. Evans, R.C. Jennings, D. Carbonera, Chlorophyll triplet states associated with Photosystem I and Photosystem II in thylakoids of the green alga *Chlamydomonas reinhardtii*, Biochim. Biophys. Acta Bioenerg. 1767 (2007) 88–105.
[72] C.P. Rijgersberg, J. Amesz, Changes in light absorbance and chlorophyll fluorescence in spinach choloplasts between 5 and 80°K, Biochim. Biophys. Acta Bioenerg. 502 (1978) 152–160.
[73] C.P. Rijgersberg, A. Melis, J. Amesz, J.A. Swager, Quenching of chlorophyll fluorescence and photochemical activity of chloroplasts at low temperature, Chlorophyll Organization and Energy Transfer in Photosynthesis Ciba Foundation Symposium, 61, Exercpta Medica, Amsterda, 1979, pp. 305–322.
[74] R. Bassi, S.Y. Soen, G. Frank, H. Zuber, J.D. Rochaix, Characterization of chlorophyll a/b proteins of photosystem I from *Chlamydomonas reinhardtii*, J. Biol. Chem. 267 (1992) 25714–25721.
[75] M. Mozzo, M. Mantelli, F. Passarini, S. Caffarri, R. Croce, R. Bassi, Functional analysis of Photosystem I light-harvesting complexes (Lhca) gene products of *Chlamydomonas reinhardtii*, Biochim. Biophys. Acta Bioenerg. 1797 (2010) 212–222.
[76] R.C. Jennings, G. Zucchelli, R. Croce, F.M. Garlaschi, The photochemical trapping rate from red spectral states in PSI-LHCI is determined by thermal activation of energy transfer to bulk chlorophylls, Biochim. Biophys. Acta Bioenerg. 1557 (2003) 91–99.